


Assessing the potential of perfect screw dislocations in SiC for solid-state quantum technologies

Daniel Barragan-Yani  and Ludger Wirtz 

Physics and Materials Science Research Unit, [University of Luxembourg](https://www.univ.lu.se/), 162a Avenue de la Faïencerie, L-1511 Luxembourg, Luxembourg

 (Received 6 June 2023; accepted 9 May 2024; published 7 June 2024)

Although point defects in solids can be used as qubits, it remains challenging to position them in a deterministic array. By means of advanced *ab initio* calculations we show that perfect screw dislocations in 3C-SiC could be used to overcome this limitation. In addition, we show that such dislocations can change the spin configuration of a point defect located inside its core, without changing the localized nature of its defect states. Our findings represent a technological leap as they show that dislocations can be used as active building blocks in future defect-based quantum computers.

DOI: [10.1103/PhysRevResearch.6.L022055](https://doi.org/10.1103/PhysRevResearch.6.L022055)

A quantum computer is a device that exploits quantum behavior to deal with computational problems that cannot be solved, or would take too long, in a classical computer [1,2]. In order to build a functioning quantum computer, several physical systems have been proposed as platforms for quantum bits (qubits), e.g., photons [3,4], trapped atoms/ions [5,6], and point defects in solids [7–12]. The latter system is advantageous from the point of view of scalability since integrated quantum devices could, in principle, be built by means of adapted fabrication techniques developed in the semiconductor industry [13]. Nevertheless, it remains challenging to position the point defects in a deterministic array and to integrate them into large networks [14].

Currently, the desired array of point defects are created using mainly irradiation and implantation. However, these methods are limited by the beam size on target (positioning accuracy of ≥ 30 nm, when achieving a high creation yield) [15–20]. As has been pointed out for the case of two-dimensional materials, alternative to more traditional methods, an engineered strain field is also able to create an array of point defects used as quantum emitters [21,22]. Nevertheless, in that case the regularity of the resulting array is hampered by the precision of the method used to grow the nanopillars that induce the strain field (positioning accuracy of 120 ± 32 nm).

Besides the localization and interconnection problems, one further limitation of current defect-based quantum technologies is that usually only point defects are considered as active elements. As a matter of fact, in their seminal work on the potential of point defects for quantum computing, Weber *et al.* proposed that one of the properties of a suitable host material would be its availability as high-quality single crystals [23]. Up to now, the presence and effects of extended defects (e.g., dislocations, stacking faults, grain boundaries, and surfaces) has been considered mostly from the point of view of

irregularities to avoid and control [12,24–36]. It was only recently that there has been interest on understanding the possible advantages and applications of extended defects, specifically stacking faults [37].

Compared to stacking faults, dislocations have a stronger and longer-range interaction with point defects due to their characteristic strain fields [39–42]. This means that, as illustrated in Fig. 1(a), qubits built using point defects could be created near an engineered dislocation and, due to the attraction between the qubits and the dislocation, an annealing process would result in a self-assembled one-dimensional array of qubits along the dislocation. Recently, it was shown that certain positions inside the cores of partial dislocations in diamond are preferred locations for NV^- centers to form, while conserving the interesting quantum properties of the centers [43]. However, partial dislocations are not radially symmetric, and several undesired configurations of the NV^- centers near partial dislocations in diamond are likely to exist [43]. One possible way to overcome these limitations and to effectively harness the potential of dislocations for quantum technologies would be to engineer perfect (undissociated) dislocations, specifically screw dislocations, which have a radially symmetric strain fields and core structures [39–42]. Another advantage of using this type of dislocation is the fact that it is possible to create ordered and regular two-dimensional arrays of perfect screw dislocations using wafer bonding techniques [44,45] and nanoindentation [46,47], which would imply the possibility of creating self-assembled two-dimensional arrays of qubits along the screw dislocations.

For this idea to work, we need host materials which satisfy two conditions: screw dislocations prefer to be undissociated and, in that preferred configuration, they are electrically inactive. The latter condition ensures that the relevant quantum properties of the defect-based qubits located along the dislocation are not altered beyond the effect of the strain field associated with the screw dislocation. Among the most relevant host materials for defect-based quantum technologies, silicon carbide is the one exhibiting perfect screw dislocations as stable configurations under normal conditions [48–50].

In this Letter, we use *ab initio* simulations to study the strength and effects of the interaction between a perfect screw

Published by the American Physical Society under the terms of the [Creative Commons Attribution 4.0 International](https://creativecommons.org/licenses/by/4.0/) license. Further distribution of this work must maintain attribution to the author(s) and the published article's title, journal citation, and DOI.

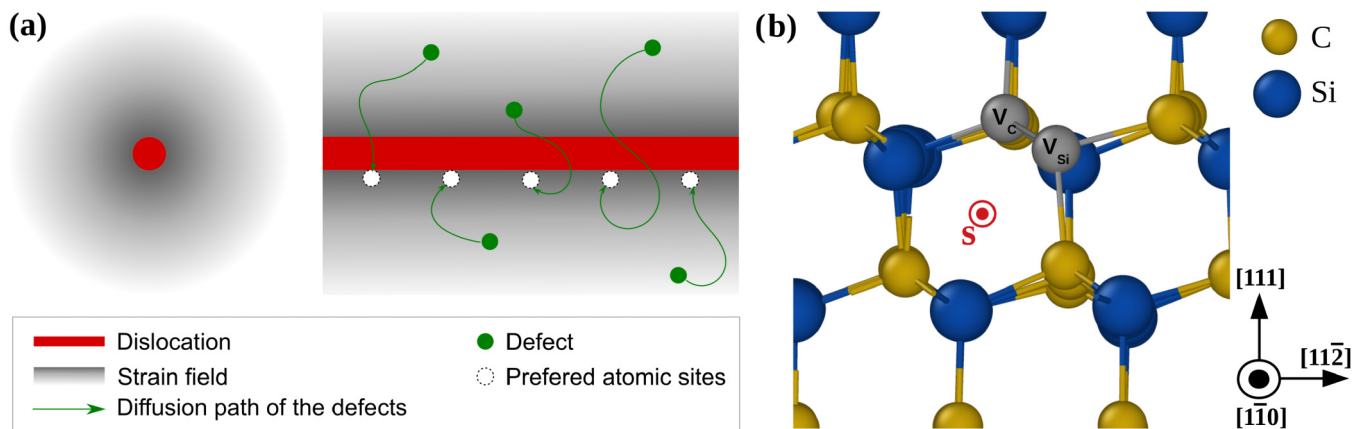


FIG. 1. (a) Depiction of a dislocation (red line) attracting defect-based qubits (green dots) due to its induced strain field (gray shaded area). Here, all preferred sites along the dislocation (white spots) are shown on one specific side of the dislocation for didactic purposes. (b) Example of the preferred configuration of the DV0 when located near a screw dislocation in 3C-SiC, i.e., both vacancies located directly at the core of the dislocation. (b) was obtained using OVITO [38].

dislocation in 3C-SiC and the divacancy (DV) in the same material. The reasons why we focus on the DV in 3C-SiC are that it is a well understood defect in 3C-SiC and that it is known to exhibit promising properties as a qubit (specifically when in its charge neutral configuration or DV0) [10,20,51,52]. To carry out our study, we analyze the change in the formation energy and electronic structure of the DV0 when located near the core of the screw dislocation. Our calculations reveal that DV0 prefers to form inside the core at specific and equivalent sites, implying that a one-dimensional array of qubits along the dislocation would be created. In addition, our results show that the same strain that drives the DV0 toward the dislocation core allows the modulation of the position of its electronic states and of its thermodynamic charge transition levels (CTLs).

Perfect screw dislocations in 3C-SiC are stable in both glide and shuffle sets [50]. Although glide cores have a lower excess energy, shuffle cores are the dislocation type expected to nucleate when creating dislocation arrays using nanoindentation techniques [49], and surface engineering could be used to also obtain them via wafer bonding [39,53]. Therefore, being most likely to occur in experiments, in this paper we focus on perfect screw dislocations in 3C-SiC that are located in the shuffle set of the 111 planes with both its dislocation line and Burgers vector lying in the $\langle 110 \rangle$ direction [48,50]. To study such dislocations in their stoichiometric and DV decorated configurations, the structural model used in our simulations contains a dislocation dipole in a quadrupolar arrangement, which minimizes the interaction between dislocations [54–56]. Such a model is created in a 576-atom SiC supercell using the software package BABEL [57]. This configuration can be seen in Fig. S1 [58] and guarantees a minimum distance between dislocation cores of ~ 16 Å. Our density functional theory (DFT) calculations are performed using the VASP [59] simulation package with a converged plane-wave energy cutoff of 500 eV. The used supercells are built with the experimental lattice parameter of 4.36 Å [60], and ions are relaxed using the Perdew-Burke-Enzerhof (PBE) [61] semilocal functional until forces are below 0.02 eV/Å. To obtain accurate formation energies,

charge transition levels, and electronic properties, we use the Heyd, Scuseria, and Enzerhof (HSE06) [62,63] hybrid functional on the PBE relaxed supercells. In all cases we use a converged $2 \times 2 \times 2$ k -point grid. To obtain a reference for our simulations, we performed calculations for the isolated DV in an analogous supercell and using the same computational setup.

Using the described methodology we tackle the first question at hand: does the DV prefer to form in the vicinity of perfect screw dislocation in 3c-SiC? To answer it, we compare the formation energy in a given charge state q of an isolated DV, $E_{\text{iso}}^f[DV^q]$, and that of the same defect when located near the core of the studied dislocation, $E_{\text{dislo}}^f[DV^q]$, which are defined as [64,65]

$$E_{\text{iso}}^f[DV^q] = E_{\text{iso}}^{\text{tot}}[DV^q] - E^{\text{tot}}[\text{bulk}] - \sum_i n_i \mu_i + q[E_F + \epsilon_{\text{VBM}}] + E_{\text{corr}}^q, \quad (1)$$

and

$$E_{\text{dislo}}^f[DV^q] = E^{\text{tot}}[(DV + \text{dislo})^q] - E^{\text{tot}}[\text{dislo}] - \sum_i n_i \mu_i + q[E_F + \epsilon_{\text{VBM}}] + E_{\text{corr}}^q, \quad (2)$$

where $E_{\text{iso}}^{\text{tot}}[DV^q]$ is the total energy of the supercell containing an isolated DV in charge state q , and $E^{\text{tot}}[(DV + \text{dislo})^q]$ is the total energy of the supercell containing the dislocation dipole with one DV, in charge state q , near one of the cores. The second term on the right side of both Eqs. (1) and (2) is the total energy of the corresponding reference supercell. In the case of the isolated DV, $E^{\text{tot}}[\text{bulk}]$ is the total energy of the pristine supercell. For the case of the DV decorated core, $E^{\text{tot}}[\text{dislo}]$ is the total energy of the supercell containing the stoichiometric dislocation dipole. The last three terms on the right in Eqs. (1) and (2) are analogous in both cases. Specifically, in the third term n_i is an integer that indicates the number of atoms of type i removed to create the DV and μ_i is the chemical potential of the same removed atoms. The fourth term, $q[E_F + \epsilon_{\text{VBM}}]$, accounts for the energy needed to charge the system. It contains the valence band maximum

(VBM) energy, E_{VBM} , and the Fermi energy, E_{F} , referenced to the VBM (i.e., their sum $E_{\text{VBM}} + E_{\text{F}}$ tell us where, inside the band gap, is the chemical potential of the electrons). The last term, E_{corr} , accounts for the correction needed to eliminate the spurious electrostatic interactions between periodic images of the defects under study. This correction is calculated using the approach proposed by Freysoldt, Neugebauer, and Van de Walle [66]. Note that this approach is only applicable if the dislocations under study are electrically inactive and all the charge added to the supercells is localized at the DVs. To prove the reliability of our methodology, in Fig. S2 it is possible to see the localized nature of the charge density difference between a DV0 and a charged DV when located directly at the core of the dislocation [58]. The charge density difference was obtained using VESTA [67].

Once $E_{\text{iso}}^{\text{f}}[DV^q]$ and $E_{\text{dislo}}^{\text{f}}[DV^q]$ are defined, we can give a quantitative estimation of the strength of the interaction between the screw dislocation and the DV by calculating

$$\Delta E^{\text{f}}[DV^q] = E_{\text{dislo}}^{\text{f}}[DV^q] - E_{\text{iso}}^{\text{f}}[DV^q], \quad (3)$$

which is negative if the DV prefers to be located near/inside the dislocation core. In the case of the neutral DV0, we found that there is a clear and strong attraction toward the dislocation. Specifically, the DV0 exhibits a $\Delta E^{\text{f}}[DV^0] = -4.2$ eV for all configurations that have both vacancies occupying sites directly at the core of the dislocation. An example of such arrangement is shown in Fig. 1(b). Our calculations show that any other configuration, with the DV0 located further away from the core, implies steep changes in the corresponding $\Delta E^{\text{f}}[DV^0]$ and a weaker interaction between the DV0 and the dislocation, i.e., a less negative $\Delta E^{\text{f}}[DV^0]$. For example, the second-preferred configuration has the silicon vacancy directly at the core and the carbon vacancy sitting outside the core, and exhibits a $\Delta E^{\text{f}}[DV^0] = -3.7$ eV. The third-preferred configuration, when both vacancies composing the DV0 are located directly outside the core and in the second ring from the center, has a $\Delta E^{\text{f}}[DV^0] = -2.6$ eV. The difference of +0.5 eV between the $\Delta E^{\text{f}}[DV^0]$ of the preferred and of the second preferred, and of +1.6 eV between the $\Delta E^{\text{f}}[DV^0]$ of the preferred and of the third-preferred configurations exemplify the strong thermodynamic driving force that pushes the DV0 toward a specific configuration along the dislocations, with both vacancies occupying sites directly at the core. Structural examples of the second- and third-preferred configurations can be seen in Fig. S3 of the Supplemental Material [58].

Although this analysis proves that the neutral DV0 is strongly attracted toward specific configurations directly at the core, a complete answer to the aforementioned question can only be given if other stable charge states are also addressed. For this purpose, we compare the CTLs of the isolated DV and those of the same defect when located near the dislocation. Besides allowing us to understand the electrical properties of defects (ionization energies), we decided to use the CTLs due to the fact that their position in the band gap provides us the stability range of the possible charge states. For a given defect, the CTLs are referred to as $\epsilon(q/q')$ and are defined as the Fermi energy values at which its formation energy for charge states q and q' become equal [64,65]. Our results

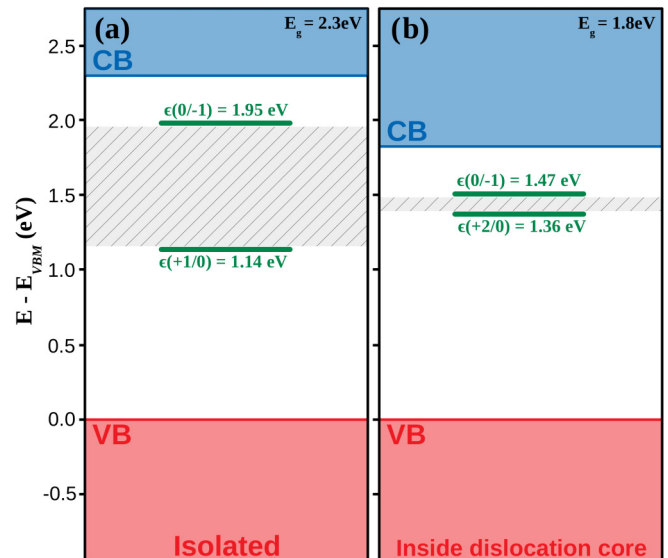


FIG. 2. Charge transition levels for the DV when (a) isolated and (b) located in its preferred configuration with both vacancies sitting directly at the core of the screw dislocation. In both figures, green horizontal lines represent the charge transition levels and dashed areas highlight the stability region for the neutral divacancy DV0. Band gaps for both cases are given on the top-right corner of each figure.

for the $\epsilon(q/q')$ are shown in Fig. 2. On the one hand, in the case of the isolated DV, we find two CTLs, $\epsilon(+1/0) = 1.14$ eV and $\epsilon(0/-1) = 1.95$ eV. This means that in 3C-SiC, the DV0 is stable in a large Fermi energy region of 0.81 eV for n -type doping conditions (around 35% of the calculated 2.36 eV band gap for bulk), which is in line with the corresponding results available in literature [68,69]. On the other hand, when the DV is located at its preferred configurations directly at the core of the screw dislocation, the stability region for the neutral DV0 is drastically reduced. In this case we found two CTLs, $\epsilon(+2/0) = 1.36$ eV and $\epsilon(0/-1) = 1.47$ eV, that imply a stability region of only 0.11 eV, which corresponds to $\sim 6\%$ of the 1.8 eV band gap obtained for a dislocated sample (the reduced band gap observed for the supercell containing the dislocation dipole is caused by the band tail states associated to the disorder induced by the dislocations [70,71]). The fact that the stability region of the DV0 is reduced despite its strong interaction with the screw dislocation with $\Delta E^{\text{f}}[DV^0] = -4.2$ eV means that the interaction between the strain induced by the dislocation and the DV in all its charge states is of the same order of magnitude but larger for higher charges, which is common to other materials and defects [72,73]. Our calculations predict that the configuration preferred by the DV0, with both vacancies sitting directly at the core of the screw dislocation, is also the preferred one for its other stable charge states. Specifically, we obtained $\Delta E^{\text{f}}[DV^{+2}] = -5.17$ eV and $\Delta E^{\text{f}}[DV^{-1}] = -4.67$ eV. These findings imply that screw dislocations in 3C-SiC are able to attract defect-based qubits and induce the formation of one-dimensional qubit arrays, but for the specific case of the DV0, the stability range of the neutral state is drastically reduced. Nevertheless, the

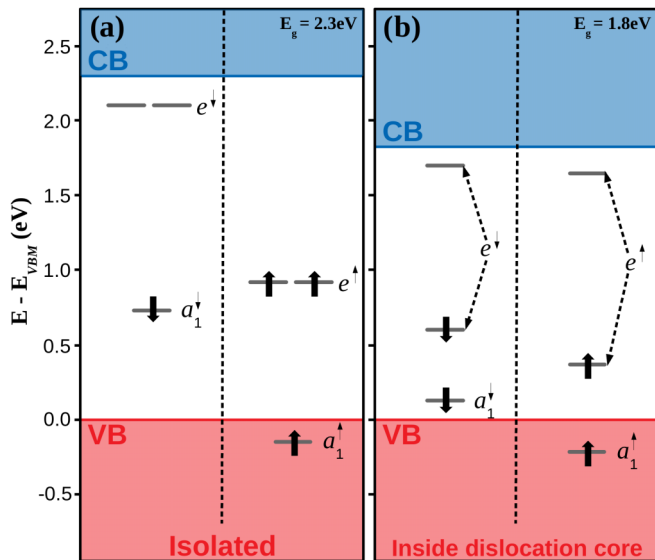


FIG. 3. Kohn-Sham states of the DV0 when (a) isolated and (b) located in its preferred configuration with both vacancies sitting directly at the core of the screw dislocation. In both figures, horizontal lines within the band gap point out the position of the obtained Kohn-Sham states and vertical arrows depict their corresponding occupations. Although the degeneracies of the $e^{\uparrow,\downarrow}$ states are lifted when the DV0 is located inside the core of the screw dislocation, for simplicity we continue to use the same labels as in the isolated case. Band gaps for both cases are given on the top-right corner of each figure.

possibility of defects with higher charge states reacting more strongly to the strain induced by the dislocation implies that new defect-based qubits, perhaps unstable in bulk, could be stabilized near screw dislocations in 3C-SiC.

At this point in our assessment we need to answer a second question: are the electronic properties that make a given defect useful as a qubit, unaltered when located in the core of the screw dislocation? Our analysis proved that, due to a reduced stability region, the DV0 would have a limited applicability when located inside the core of the screw dislocation. Nevertheless, we can study its Kohn-Sham states to reveal the effect of the strain field induced by the dislocation on the electronic structure of a potential qubit. In line with available literature on the matter [68,74,75], our calculations show that the isolated DV0 introduces an occupied a_1^{\downarrow} state, a doubly occupied and degenerate e^{\uparrow} state, and an unoccupied and degenerate e^{\downarrow} state within the band gap of bulk 3C-SiC [see Fig. 3(a)]. In addition, we also find an occupied a_1^{\downarrow} state just below the valence band maximum. Altogether, the induced states imply a $S = 1$ spin triplet ground state for the isolated DV, and its electronic structure satisfies the criteria required for

defect-based qubits [23]. As can be seen in Fig. 3(b), in the case of the DV0 located in its preferred configuration inside the screw dislocation core, the degeneracy of the $e^{\uparrow,\downarrow}$ states is lifted. The cause of this change is the localized disorder near the cores, which can be understood using a coordination analysis for the region near the core (see Fig. S4 [58]). This same disorder is the cause of the band tail states that reduce the band gap in the dislocated supercell [70,71]). The consequence of the degeneracy being lifted is that, compared to the isolated DV0, the DV0 near the core does not introduce a doubly occupied e^{\uparrow} state, but a singly occupied e^{\downarrow} state and a singly occupied e^{\uparrow} state. Together with the occupied $a_1^{\uparrow,\downarrow}$, which are common to both the isolated and inside-the-core DV0, the electronic structure shown in Fig. 3(b) implies a $S = 0$ spin singlet. This means that, besides seeing its stability region reduced, the DV0 located inside the core of the screw dislocation is not useful as a qubit. However, as it can also be seen in Fig. 3(b), the screw dislocation does not induce any deep state by itself and it allows a defect sitting in its core to have bound states. These findings imply that new defect-based qubits, perhaps useless in bulk, could become paramagnetic by having their electronic degeneracy being lifted near screw dislocations in 3C-SiC.

In conclusion, we propose that, in order to have potential for quantum applications, dislocations should be undissociated screws and be electrically inactive. Such conditions are satisfied in 3C-SiC, and our calculations show that the undissociated screw dislocation in this material is able to attract defect-based qubits into its core. As a consequence, it would allow the creation of a one-dimension array of qubits along its line direction. Furthermore, we show that the strain field induced by this specific dislocation type is able to modulate both, the charge transition levels and the electronic structure of the qubit located in its core, without itself being electrically active. For the DV0, which is chosen as first study case due to its experimentally proven potential as qubit in 3C-SiC, our results show that these modulations result in the loss of its potential as a qubit. However, our results call for further calculations to check whether the same modulations could transform defects with no potential as qubits when located in bulk, into promising options when located inside the core of the screw dislocations. Altogether our findings represent a paradigm shift within quantum technologies, as they point out that perfect screw dislocations can be used as active building blocks of future defect-based quantum computers.

We acknowledge that this project has received funding from the European Union's Horizon 2020 research and innovation programme under the Marie Skłodowska-Curie Grant Agreement No. 898860. Furthermore, the authors gratefully acknowledge the computing time granted by the HPC facilities of the University of Luxembourg and the HRZ (Lichtenberg-Cluster) at TU Darmstadt.

[1] M. A. Nielsen and I. L. Chuang, *Quantum Computation and Quantum Information: 10th Anniversary Edition* (Cambridge University Press, Cambridge, 2010).

[2] T. D. Ladd, F. Jelezko, R. Laflamme, Y. Nakamura, C. Monroe, and J. L. O'Brien, Quantum computers, *Nature (London)* **464**, 45 (2010).

- [3] F. Flamini, N. Spagnolo, and F. Sciarrino, Photonic quantum information processing: A review, *Rep. Prog. Phys.* **82**, 016001 (2019).
- [4] S. Slussarenko and G. J. Pryde, Photonic quantum information processing: A concise review, *Appl. Phys. Rev.* **6**, 041303 (2019).
- [5] H. Häffner, C. F. Roos, and R. Blatt, Quantum computing with trapped ions, *Phys. Rep.* **469**, 155 (2008).
- [6] C. D. Bruzewicz, J. Chiaverini, R. McConnell, and J. M. Sage, Trapped-ion quantum computing: Progress and challenges, *Appl. Phys. Rev.* **6**, 021314 (2019).
- [7] A. Gruber, A. Dräbenstedt, C. Tietz, L. Fleury, J. Wrachtrup, and C. von Borczyskowski, Scanning confocal optical microscopy and magnetic resonance on single defect centers, *Science* **276**, 2012 (1997).
- [8] G. Balasubramanian, P. Neumann, D. Twitchen, M. Markham, R. Kolesov, N. Mizuochi, J. Isoya, J. Achard, J. Beck, J. Tisler, V. Jacques, P. R. Hemmer, F. Jelezko, and J. Wrachtrup, Ultra-long spin coherence time in isotopically engineered diamond, *Nat. Mater.* **8**, 383 (2009).
- [9] M. W. Doherty, N. B. Manson, P. Delaney, F. Jelezko, J. Wrachtrup, and L. C. L. Hollenberg, The nitrogen-vacancy colour centre in diamond, *Phys. Rep.* **528**, 1 (2013).
- [10] G. Zhang, Y. Cheng, J.-P. Chou, and A. Gali, Material platforms for defect qubits and single-photon emitters, *Appl. Phys. Rev.* **7**, 031308 (2020).
- [11] A. Chatterjee, P. Stevenson, S. De Franceschi, A. Morello, N. P. de Leon, and F. Kuemmeth, Semiconductor qubits in practice, *Nat. Rev. Phys.* **3**, 157 (2021).
- [12] G. Wolfowicz, F. J. Heremans, C. P. Anderson, S. Kanai, H. Seo, A. Gali, G. Galli, and D. D. Awschalom, Quantum guidelines for solid-state spin defects, *Nat. Rev. Mater.* **6**, 906 (2021).
- [13] W. F. Koehl, H. Seo, G. Galli, and D. D. Awschalom, Designing defect spins for wafer-scale quantum technologies, *MRS Bull.* **40**, 1146 (2015).
- [14] M. Atatüre, D. Englund, N. Vamivakas, S.-Y. Lee, and J. Wrachtrup, Material platforms for spin-based photonic quantum technologies, *Nat. Rev. Mater.* **3**, 38 (2018).
- [15] T. Schröder, M. E. Trusheim, M. Walsh, L. Li, J. Zheng, M. Schukraft, A. Sipahigil, R. E. Evans, D. D. Sukachev, C. T. Nguyen, J. L. Pacheco, R. M. Camacho, E. S. Bielejec, M. D. Lukin, and D. Englund, Scalable focused ion beam creation of nearly lifetime-limited single quantum emitters in diamond nanostructures, *Nat. Commun.* **8**, 15376 (2017).
- [16] J. Wang, Y. Zhou, X. Zhang, F. Liu, Y. Li, K. Li, Z. Liu, G. Wang, and W. Gao, Efficient generation of an array of single silicon-vacancy defects in silicon carbide, *Phys. Rev. Appl.* **7**, 064021 (2017).
- [17] Y. Zhou, Z. Mu, G. Adamo, S. Bauerdick, A. Rudzinski, I. Aharonovich, and W. bo Gao, Direct writing of single germanium vacancy center arrays in diamond, *New J. Phys.* **20**, 125004 (2018).
- [18] Y.-C. Chen, B. Griffiths, L. Weng, S. S. Nicley, S. N. Ishmael, Y. Lekhai, S. Johnson, C. J. Stephen, B. L. Green, G. W. Morley, M. E. Newton, M. J. Booth, P. S. Salter, and J. M. Smith, Laser writing of individual nitrogen-vacancy defects in diamond with near-unity yield, *Optica* **6**, 662 (2019).
- [19] J. M. Smith, S. A. Meynell, A. C. Bleszynski Jayich, and J. Meijer, Colour centre generation in diamond for quantum technologies, *Nanophotonics* **8**, 1889 (2019).
- [20] S. Castelletto and A. Boretti, Silicon carbide color centers for quantum applications, *J. Phys.: Photonics* **2**, 022001 (2020).
- [21] S. Kumar, A. Kaczmarczyk, and B. D. Gerardot, Strain-induced spatial and spectral isolation of quantum emitters in mono- and bilayer WSe₂, *Nano Lett.* **15**, 7567 (2015).
- [22] A. Branny, S. Kumar, R. Proux, and B. D. Gerardot, Deterministic strain-induced arrays of quantum emitters in a two-dimensional semiconductor, *Nat. Commun.* **8**, 15053 (2017).
- [23] J. R. Weber, W. F. Koehl, J. B. Varley, A. Janotti, B. B. Buckley, C. G. Van de Walle, and D. D. Awschalom, Quantum computing with defects, *Proc. Natl. Acad. Sci. USA* **107**, 8513 (2010).
- [24] P. C. E. Stamp and A. Gaita-Ariño, Spin-based quantum computers made by chemistry: Hows and whys, *J. Mater. Chem.* **19**, 1718 (2009).
- [25] L. C. Bassett, A. Alkauskas, A. L. Exarhos, and K.-M. C. Fu, Quantum defects by design, *Nanophotonics* **8**, 1867 (2019).
- [26] M. Kaviani, P. Deák, B. Aradi, T. Frauenheim, J.-P. Chou, and A. Gali, Proper surface termination for luminescent near-surface NV centers in diamond, *Nano Lett.* **14**, 4772 (2014).
- [27] J.-P. Chou and A. Gali, Nitrogen-vacancy diamond sensor: novel diamond surfaces from *ab initio* simulations, *MRS Commun.* **7**, 551 (2017).
- [28] J.-P. Chou, A. Retzker, and A. Gali, Nitrogen-terminated diamond (111) surface for room-temperature quantum sensing and simulation, *Nano Lett.* **17**, 2294 (2017).
- [29] A. Stacey, N. Dontschuk, J.-P. Chou, D. A. Broadway, A. K. Schenk, M. J. Sear, J.-P. Tetienne, A. Hoffman, S. Prawer, C. I. Pakes, A. Tadich, N. P. de Leon, A. Gali, and L. C. L. Hollenberg, Evidence for primal sp² defects at the diamond surface: Candidates for electron trapping and noise sources, *Adv. Mater. Inter.* **6**, 1801449 (2019).
- [30] S. Sangtawesin, B. L. Dwyer, S. Srinivasan, J. J. Allred, L. V. H. Rodgers, K. De Greve, A. Stacey, N. Dontschuk, K. M. O'Donnell, D. Hu, D. A. Evans, C. Jaye, D. A. Fischer, M. L. Markham, D. J. Twitchen, H. Park, M. D. Lukin, and N. P. de Leon, Origins of diamond surface noise probed by correlating single-spin measurements with surface spectroscopy, *Phys. Rev. X* **9**, 031052 (2019).
- [31] S. Li, J.-P. Chou, J. Wei, M. Sun, A. Hu, and A. Gali, Oxygenated (113) diamond surface for nitrogen-vacancy quantum sensors with preferential alignment and long coherence time from first principles, *Carbon* **145**, 273 (2019).
- [32] W. Shen, S. Shen, S. Liu, H. Li, Z. Gan, and Q. Zhang, Monolayer cubic boron nitride terminated diamond (111) surfaces for quantum sensing and electron emission applications, *ACS Appl. Mater. Interfaces* **12**, 33336 (2020).
- [33] W. Körner, D. F. Urban, and C. Elsässer, Influence of extended defects on the formation energy, hyperfine structure, and zero-field splitting of NV centers in diamond, *Phys. Rev. B* **103**, 085305 (2021).
- [34] W. Körner, R. Ghassemizadeh, D. F. Urban, and C. Elsässer, Influence of (N,H)-terminated surfaces on stability, hyperfine structure, and zero-field splitting of NV centers in diamond, *Phys. Rev. B* **105**, 085305 (2022).

- [35] R. Löfgren, S. Öberg, and J. A. Larsson, The diamond NV-center transition energies in the vicinity of an intrinsic stacking fault, *AIP Adv.* **12**, 035009 (2022).
- [36] B. L. Dwyer, L. V. H. Rodgers, E. K. Urbach, D. Bluvstein, S. Sangtawesin, H. Zhou, Y. Nassab, M. Fitzpatrick, Z. Yuan, K. De Greve, E. L. Peterson, H. Knowles, T. Sumarac, J.-P. Chou, A. Gali, V. V. Dobrovitski, M. D. Lukin, and N. P. de Leon, Probing spin dynamics on diamond surfaces using a single quantum sensor, *PRX Quantum* **3**, 040328 (2022).
- [37] V. Ivády, J. Davidsson, N. Deegan, A. L. Falk, P. V. Klimov, S. J. Whiteley, S. O. Hruszkewycz, M. V. Holt, F. J. Heremans, N. T. Son, D. D. Awschalom, I. A. Abrikosov, and A. Gali, Stabilization of point-defect spin qubits by quantum wells, *Nat. Commun.* **10**, 5607 (2019).
- [38] A. Stukowski, Visualization and analysis of atomistic simulation data with ovito—the open visualization tool, *Modell. Simul. Mater. Sci. Eng.* **18**, 015012 (2010).
- [39] D. B. Holt and B. G. Yacobi, *Extended Defects in Semiconductors: Electronic Properties, Device Effects and Structures* (Cambridge University Press, Cambridge, 2007).
- [40] D. Hull and D. J. Bacon, *Introduction to Dislocations*, Materials science and technology (Elsevier Science, Oxford, 2011).
- [41] W. Cai, W. D. Nix, and M. R. Society, *Imperfections in Crystalline Solids*, MRS-Cambridge Materials Fundamentals (Cambridge University Press, Cambridge, 2016).
- [42] P. M. Anderson, J. P. Hirth, and J. Lothe, *Theory of Dislocations* (Cambridge University Press, Cambridge, 2017).
- [43] R. Ghassemizadeh, W. Körner, D. F. Urban, and C. Elsässer, Stability and electronic structure of NV centers at dislocation cores in diamond, *Phys. Rev. B* **106**, 174111 (2022).
- [44] M. Reiche, M. Kittler, D. Buca, A. Hähnel, Q.-T. Zhao, S. Mantl, and U. Gösele, Dislocation-based Si-nanodevices, *Jpn. J. Appl. Phys.* **49**, 04DJ02 (2010).
- [45] M. Reiche, M. Kittler, W. Erfurth, E. Pippel, K. Sklarek, H. Blumtritt, A. Haehnel, and H. Uebensee, On the electronic properties of a single dislocation, *J. Appl. Phys.* **115**, 194303 (2014).
- [46] S. Kondo, T. Mitsuma, N. Shibata, and Y. Ikuhara, Direct observation of individual dislocation interaction processes with grain boundaries, *Sci. Adv.* **2**, e1501926 (2016).
- [47] H. Bishara, H. Tsybenko, S. Nandy, Q. K. Muhammad, T. Frömling, X. Fang, J. P. Best, and G. Dehm, Dislocation-enhanced electrical conductivity in rutile TiO₂ accessed by room-temperature nanoindentation, *Scr. Mater.* **212**, 114543 (2022).
- [48] L. Pizzagalli, P. Beauchamp, and J. Rabier, Stability of undissociated screw dislocations in zinc-blende covalent materials from first-principle simulations, *Europhys. Lett.* **72**, 410 (2005).
- [49] J.-L. Demenet, M. Amer, C. Tromas, D. Eyidi, and J. Rabier, Dislocations in 4H- and 3C-SiC single crystals in the brittle regime, *Phys. Status Solidi C* **10**, 64 (2013).
- [50] L. Pizzagalli, Stability and mobility of screw dislocations in 4h, 2H and 3C silicon carbide, *Acta Mater.* **78**, 236 (2014).
- [51] D. J. Christle, P. V. Klimov, C. F. de las Casas, K. Szász, V. Ivády, V. Jokubavicius, J. Ul Hassan, M. Syväjärvi, W. F. Koehl, T. Ohshima, N. T. Son, E. Janzén, Á. Gali, and D. D. Awschalom, Isolated spin qubits in SiC with a high-fidelity infrared spin-to-photon interface, *Phys. Rev. X* **7**, 021046 (2017).
- [52] N. T. Son, C. P. Anderson, A. Bourassa, K. C. Miao, C. Babin, M. Widmann, M. Niethammer, J. Ul Hassan, N. Morioka, I. G. Ivanov, F. Kaiser, J. Wrachtrup, and D. D. Awschalom, Developing silicon carbide for quantum spintronics, *Appl. Phys. Lett.* **116**, 190501 (2020).
- [53] S. Wang, *Lattice Engineering: Technology and Applications* (Pan Stanford, Singapore, 2012).
- [54] V. Bulatov and W. Cai, *Computer Simulations of Dislocations*, OSMM (OUP Oxford, Oxford, 2006).
- [55] D. Rodney, L. Ventelon, E. Clouet, L. Pizzagalli, and F. Willaime, *Ab initio* modeling of dislocation core properties in metals and semiconductors, *Acta Mater.* **124**, 633 (2017).
- [56] E. Clouet, *Ab initio* models of dislocations, in *Handbook of Materials Modeling: Methods: Theory and Modeling*, edited by W. Andreoni and S. Yip (Springer International Publishing, Cham, Switzerland, 2020), pp. 1503–1524.
- [57] E. Clouet, Babel package. Available online at URL <http://emmanuel.clouet.free.fr/Programs/Babel/>.
- [58] See Supplemental Material at <http://link.aps.org/supplemental/10.1103/PhysRevResearch.6.L022055> for details about the used supercells containing the dislocation dipoles, the charge transfer between the DV and the dislocation, examples of configurations of the DV located near the screw dislocation but outside its core, and the coordination analysis of the dislocated supercell.
- [59] G. Kresse and J. Furthmüller, Efficient iterative schemes for *ab initio* total-energy calculations using a plane-wave basis set, *Phys. Rev. B* **54**, 11169 (1996).
- [60] Z. Li and R. C. Bradt, Thermal expansion of the cubic (3C) polytype of SiC, *J. Mater. Sci.* **21**, 4366 (1986).
- [61] J. P. Perdew, K. Burke, and M. Ernzerhof, Generalized gradient approximation made simple, *Phys. Rev. Lett.* **77**, 3865 (1996).
- [62] J. Heyd, G. E. Scuseria, and M. Ernzerhof, Hybrid functionals based on a screened coulomb potential, *J. Chem. Phys.* **118**, 8207 (2003).
- [63] J. Heyd, G. E. Scuseria, and M. Ernzerhof, Erratum: “hybrid functionals based on a screened coulomb potential” [*J. chem. phys.* 118, 8207 (2003)], *J. Chem. Phys.* **124**, 219906 (2006).
- [64] C. Freysoldt, B. Grabowski, T. Hickel, J. Neugebauer, G. Kresse, A. Janotti, and C. G. Van de Walle, First-principles calculations for point defects in solids, *Rev. Mod. Phys.* **86**, 253 (2014).
- [65] H.-P. Komsa, T. T. Rantala, and A. Pasquarello, Finite-size supercell correction schemes for charged defect calculations, *Phys. Rev. B* **86**, 045112 (2012).
- [66] C. Freysoldt, J. Neugebauer, and C. G. Van de Walle, Fully *ab initio* finite-size corrections for charged-defect supercell calculations, *Phys. Rev. Lett.* **102**, 016402 (2009).
- [67] K. Momma and F. Izumi, VESTA3 for three-dimensional visualization of crystal, volumetric and morphology data, *J. Appl. Crystallogr.* **44**, 1272 (2011).
- [68] L. Gordon, A. Janotti, and C. G. Van de Walle, Defects as qubits in 3C- and 4H-SiC, *Phys. Rev. B* **92**, 045208 (2015).
- [69] P. A. Schultz, R. M. Van Ginhoven, and A. H. Edwards, Theoretical study of intrinsic defects in cubic silicon carbide 3C-SiC, *Phys. Rev. B* **103**, 195202 (2021).
- [70] S. M. Lee, M. A. Belkhir, X. Y. Zhu, Y. H. Lee, Y. G. Hwang, and T. Frauenheim, Electronic structures of GaN edge dislocations, *Phys. Rev. B* **61**, 16033 (2000).
- [71] D. Barragan-Yani and K. Albe, Atomic and electronic structure of perfect dislocations in the solar absorber materials CuInSe₂

- and CuGaSe₂ studied by first-principles calculations, *Phys. Rev. B* **95**, 115203 (2017).
- [72] U. Aschauer and N. A. Spaldin, Interplay between strain, defect charge state, and functionality in complex oxides, *Appl. Phys. Lett.* **109**, 031901 (2016).
- [73] E. Simsek Sanli, D. Barragan-Yani, Q. M. Ramasse, K. Albe, R. Mainz, D. Abou-Ras, A. Weber, H.-J. Kleebe, and P. A. van Aken, Point defect segregation and its role in the detrimental nature of Frank partials in Cu(In,Ga) Se₂ thin-film absorbers, *Phys. Rev. B* **95**, 195209 (2017).
- [74] A. Csóré, N. Mukesh, G. Károlyházy, D. Beke, and A. Gali, Photoluminescence spectrum of divacancy in porous and nanocrystalline cubic silicon carbide, *J. Appl. Phys.* **131**, 071102 (2022).
- [75] W. Gao, F. H. da Jornada, M. Del Ben, J. Deslippe, S. G. Louie, and J. R. Chelikowsky, Quasiparticle energies and optical excitations of 3C-SiC divacancy from *GW* and *GW* plus bethe-salpeter equation calculations, *Phys. Rev. Mater.* **6**, 036201 (2022).